

A CT-based radiomics nomogram for prediction of human epidermal growth factor receptor 2 status in patients with gastric cancer

Yexing Li^{1,2*}, Zixuan Cheng^{1,3*}, Olivier Gevaert^{4*}, Lan He¹, Yanqi Huang¹, Xin Chen^{1,5,6}, Xiaomei Huang^{1,5}, Xiaomei Wu^{1,3}, Wen Zhang^{1,5,7}, Mengyi Dong^{1,5}, Jia Huang^{1,2}, Yucun Huang^{1,5,8}, Ting Xia^{1,3}, Changhong Liang^{1,2}, Zaiyi Liu^{1,2}

¹Department of Radiology, Guangdong Provincial People's Hospital, Guangdong Academy of Medical Sciences, Guangzhou 510080, China; ²Graduate College, Shantou University Medical College, Shantou 515041, China; ³School of Medicine, South China University of Technology, Guangzhou 510006, China; ⁴Stanford Center for Biomedical Informatics Research, Department of Medicine, and Department of Biomedical Data Science, Stanford University, California 94305, USA; ⁵Graduate College, Southern Medical University, Guangzhou 510515, China; ⁶Department of Radiology, Guangzhou First People's Hospital, Guangzhou 510180, China; ⁷Department of Radiology, Zhuhai Hospital of Traditional Chinese and Western Medicine, Zhuhai 519000, China; ⁸Department of Radiology, The Fifth People's Hospital of Zhuhai, Zhuhai 519055, China

*These authors contributed equally to this work.

Correspondence to: Changhong Liang, PhD. Department of Radiology, Guangdong Provincial People's Hospital, Guangdong Academy of Medical Sciences, No.106 Zhongshan Er Road, Guangzhou 510080, China. Email: cjr.lchh@vip.163.com; Zaiyi Liu, PhD. Department of Radiology, Guangdong Provincial People's Hospital, Guangdong Academy of Medical Sciences, No.106 Zhongshan Er Road, Guangzhou 510080, China. Email: zyliu@163.com.

Abstract

Objective: To develop and validate a computed tomography (CT)-based radiomics nomogram for predicting human epidermal growth factor receptor 2 (HER2) status in patients with gastric cancer.

Methods: This retrospective study included 134 patients with gastric cancer (HER2-negative: n=87; HER2-positive: n=47) from April 2013 to March 2018, who were then randomly divided into training (n=94) and validation (n=40) cohorts. Radiomics features were obtained from the CT images showing gastric cancer. Least absolute shrinkage and selection operator (LASSO) regression analysis was utilized for building the radiomics signature. A multivariable logistic regression method was applied to develop a prediction model incorporating the radiomics signature and independent clinicopathologic risk predictors, which were then visualized as a radiomics nomogram. The predictive performance of the nomogram was assessed in the training and validation cohorts.

Results: The radiomics signature was significantly associated with HER2 status in both training ($P<0.001$) and validation ($P=0.023$) cohorts. The prediction model that incorporated the radiomics signature and carcinoembryonic antigen (CEA) level demonstrated good discriminative performance for HER2 status prediction, with an area under the curve (AUC) of 0.799 [95% confidence interval (95% CI): 0.704–0.894] in the training cohort and 0.771 (95% CI: 0.607–0.934) in the validation cohort. The calibration curve of the radiomics nomogram also showed good calibration. Decision curve analysis showed that the radiomics nomogram was useful.

Conclusions: We built and validated a radiomics nomogram with good performance for HER2 status prediction in gastric cancer. This radiomics nomogram could serve as a non-invasive tool to predict HER2 status and guide clinical treatment.

Keywords: Gastric cancer; human epidermal growth factor receptor 2; radiomics; X ray; computed tomography

Submitted Sep 08, 2019. Accepted for publication Dec 03, 2019.

doi: 10.21147/j.issn.1000-9604.2020.01.08

View this article at: <https://doi.org/10.21147/j.issn.1000-9604.2020.01.08>

Introduction

Gastric cancer remains one of the most common tumors globally, especially in eastern Asia (1). Although its incidence and mortality rates have been declining steadily in many countries, they still rank the fifth and third, respectively (2). According to the global cancer statistics, there would be approximately 1.0 million new cases and 723,000 deaths attributable to gastric cancer globally in 2018, China shows a particularly high incidence of gastric cancer, accounting for 40% of the cases worldwide (1-3). Radical gastrectomy remains the only curative approach for gastric cancer. The combination of surgical resection with adjuvant chemotherapy and chemoradiation is the main treatment procedure for advanced gastric cancer according to the National Comprehensive Cancer Network guidelines (4). However, the prognosis remains poor after treatment for patients with advanced gastric cancer (5,6).

Previous studies have demonstrated that the pathogenesis and poor outcomes of advanced gastric and gastroesophageal junction cancer were related to the status of human epidermal growth factor receptor 2 (HER2, currently known as ERBB2, but referred to as HER2 in this study), and 6%–30% of gastric cancer cases were reported to show a HER2-positive status (7). Many studies have also shown that HER2 overexpression is a biomarker and a key driver of tumorigenesis as well as a prognostic factor in gastric cancer (7-9). In comparison with established chemotherapy alone, chemotherapy with the addition of the anti-HER2 antibody trastuzumab resulted in prolonged survival and improved outcomes in HER2-positive advanced gastric or gastroesophageal junction cancer (8). HER2-positive gastric cancer patients may thus benefit from targeted therapy with trastuzumab, and therefore, timely and accurate determination of HER2 status plays an important role in the treatment of gastric cancer (8,10).

In clinical practice, the HER2 status is primarily evaluated by immunohistochemistry (IHC) or fluorescence *in situ* hybridization (FISH), which is the invasive method involving tissue samples (7,11). As a result, HER2 status retest or follow-up assessments during the treatment process are not routinely performed for patients with gastric cancer. Although some studies have explored the possibility of noninvasively predicting HER2 status with positron emission tomography (PET) imaging, their reported predictive abilities were not consistent (12,13). Therefore, there is an urgent need for new methods to evaluate the HER2 status of gastric cancer.

Computed tomography (CT) is a routine imaging modality for the diagnosis, treatment evaluation, and postoperative follow-up of gastric cancer, and has been widely used in clinical practice (14). Nevertheless, there are no studies that have attempted to preoperatively predict HER2 status on the basis of CT analysis. Radiomics, which is defined as the extraction of quantitative image features for further analysis to support clinical decision-making, has been applied for diagnosis and evaluation of the treatment efficacy and prognosis of tumors (15-19). Radiomics based on CT images has been performed in cases of gastric cancer and shows potential for guiding clinical decision-making for patients (19,21). Thus, radiomics may provide a new approach for simple, non-invasive and repeatable prediction of HER2 status at the low costs of routinely acquired CT images (18). Therefore, the purpose of this study was to develop a CT-based radiomics nomogram to predict HER2 status in patients with gastric cancer and provide preliminary performance testing.

Materials and methods

Patients

Ethical approval for this study was obtained from Guangdong Provincial People's Hospital and the requirement for informed consent was waived since this was a retrospective analysis. A total of 134 patients with gastric cancer underwent pre-treatment contrast-enhanced CT examination from April 2013 to March 2018 at Guangdong Provincial People's Hospital.

The inclusion criteria of this study were 1) contrast-enhanced CT examination within a month before gastrectomy; 2) visible tumor lesions on CT images judged by two experienced radiologists; 3) gastric adenocarcinoma confirmed on postoperative pathological examination; 4) HER2 status tested by FISH after gastrectomy; and 5) no preoperative radiotherapy or chemotherapy. All 134 cases were randomly divided into the training cohort [n=94 (HER2-negative: 62, HER2-positive: 32)], and the validation cohort [n=40 (HER2-negative: 25, HER2-positive: 15)].

We collected data for the following clinicopathologic characteristics: sex, age, clinical stage, CT-reported T stage, HER2 status, preoperative carcinoembryonic antigen (CEA) level, and tumor location. Laboratory analysis of CEA levels was performed through routine blood tests within 1 week before surgical operation. According to the

standards used at Guangdong Provincial People's Hospital, a normal CEA level was defined as ≤ 5 ng/mL and an abnormal CEA level was defined as >5 ng/mL. The tumor location was categorized as upper-third, middle-third and lower-third according to the main location of the lesions. The clinical stage and CT-reported T stage were classified using CT images according to the 8th American Joint Committee on Cancer (AJCC) staging system (14). CT-reported T stage of gastric cancer was categorized into two stages (T1–2, T3–4).

HER2 status determination

The HER2 status was tested via FISH examinations within a week after gastrectomy. The HER2 status in gastric cancer mainly depends on the ratio between the average number of HER2 signals and chromosome enumeration probe 17 (CEP17) signals (HER2/CEP17) in FISH (22). The HER2 status of gastric cancer in Guangdong Provincial People's Hospital was defined to be positive if the HER2/CEP17 ratio was ≥ 2 , whereas the status was considered negative if the HER2/CEP17 ratio was <2 .

CT image acquisition protocol

All patients fasted for more than 5 h and were asked to drink 600–1,000 mL of water before the CT scan. An abdominal contrast-enhanced CT was performed with multidetector row CT (MDCT) scanners, which covered the whole stomach region. The CT scanning parameters are shown in *Supplementary Table S1*.

After injection of 1.5 mL/kg of iodinated contrast material (Ultravist 370; Bayer Schering Pharma, Berlin, Germany) with an automatic power pump injector (Ulrich CT Plus 150; Ulrich Medical, Ulm, Germany) at a rate of 3.5 mL/s into the antecubital vein, CT images in the

arterial and portal venous phase were respectively obtained at a 30 s and 60 s delay after infusion of contrast material.

Radiomics feature extraction

CT images were retrieved from the picture archiving and communication system (Carestream, Canada). Since a majority of gastric tumor lesions showed significant enhancement in the portal venous phase and facilitated discrimination between tumor masses and perigastric tissues (23), the CT images of this phase were selected for tumor segmentation as described previously (24). Manual segmentation was performed with ITK-SNAP software (Version 3.6.0, <http://www.itksnap.org>) to obtain the region of interest (ROI) for radiomics analysis. ROIs were manually drawn to outline the visible tumor and integrated as a volume of interest (VOI); the details are shown in *Figure 1*. CT images of all patients were then fed into an in-house script based on MATLAB 2016b (MathWorks, Natick, MA) to extract the radiomics features, which contains first-order statistics, texture features, size- and shape-based features, and wavelet features (*Supplementary materials*).

The VOIs of all patients were delineated by an experienced radiologist (reader 1) with 5 years of experience in gastrointestinal CT interpretation. To verify the intraobserver and interobserver reproducibility, 40 patients were randomly chosen from among all 134 cases, and VOI delineation and radiomics feature extraction were repeated by reader 1 and then performed again by another experienced radiologist (reader 2) with 10 years of experience in gastrointestinal CT interpretation a month later (24,25). Intragastric air, necrosis area, enlarged lymph nodes, and perigastric adipose tissue were removed from the VOIs as described before (24).

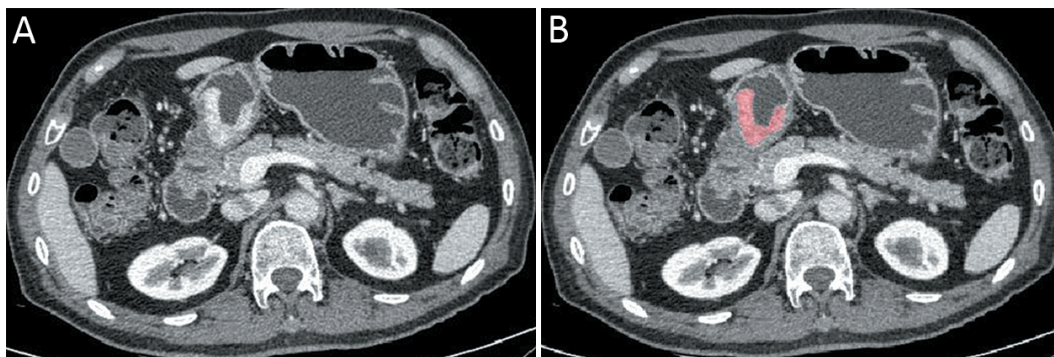


Figure 1 An example of manual segmentation in gastric cancer. (A) Localized thick wall of gastric cancer with enhancement is observed on the portal venous phase computed tomography (CT) image; (B) Manual segmentation on the same axial slice is depicted with red label.

Radiomics feature selection and radiomics signature building

Intraclass correlation coefficient (ICC) values were applied to assess the stability and robustness of radiomics feature extraction. The intraobserver ICC was computed on the basis of the repeated feature extraction by reader 1, while the interobserver ICC was obtained on the basis of the first feature extraction performed by reader 1 and the extraction performed by reader 2. We generally interpreted ICCs of >0.75 as indicating almost excellent agreement in reproducibility (26). We excluded highly correlated features by using the following approach. Spearman's correlation coefficient between each pair of features was calculated, and feature pairs with coefficients greater than 0.9 were deemed highly correlated and one of the two features was excluded. All the remaining features were standardized with z-score normalization in both training and validation cohorts by using the mean and standard deviation values from the feature data in the training cohort. The least absolute shrinkage and selection operator (LASSO) logistic regression analysis method, which is used to perform high-dimensional data regression analysis, was used to explore the relationship between stable radiomics features and HER2 status. The LASSO logistic regression method selected optimal features and then combined them to build a radiomics signature in the training cohort. The radiomics score (Rad-score) of each patient was calculated by determining the product of the selected features' linear combinations and their respective coefficients.

Predictive performance of radiomics signature

The performance of the radiomics signature for prediction of HER2 status was evaluated in the training cohort and then validated in the validation cohort. The receiver operating characteristic (ROC) curve was applied to evaluate the discrimination of the radiomics signature.

Construction of radiomics nomogram

Multivariable logistic regression analysis was performed to develop a prediction model by combining the radiomics signature and clinicopathologic predictors with P values less than 0.1 in the univariable analysis. In order to promote the clinical application value of the prediction model, we visualized the model as a radiomics nomogram based on multivariable logistic analysis in the training cohort.

Predictive performance of radiomics nomogram

The ROC curve was used to assess the discriminative performance of the radiomics nomogram. A calibration curve was applied to assess the radiomics nomogram. Decision curve analysis (DCA) was performed to estimate the clinical usefulness of the radiomics nomogram by calculating the net benefits at a range of threshold probabilities in the training cohort. Additionally, we determined the net reclassification improvement (NRI) to compare the predictive performance of the radiomics signature and nomogram.

Statistical analysis

We used IBM SPSS Statistics (Version 20.0; IBM Corp., New York, USA) to analyze the clinical data in this study. Mann-Whitney U tests were used to evaluate the differences in age between patients in the training and validation cohorts, and the Chi-square test was used to analyze categorical variables, such as sex, clinical stage, CT-reported T stage, tumor location, and CEA level in the two cohorts. The age of patients with gastric cancer as a continuous variable was expressed as the $\bar{x} \pm s$. The association between Rad-score and HER2 status was also assessed by the Mann-Whitney U test in the training and validation cohorts. R software (Version 3.3.1; R Foundation for Statistical Computing, Vienna, Austria, <http://www.R-project.org>) was used to analyze the radiomics feature data. Packages of R software used in this study are listed in *Supplementary materials*. A $P < 0.05$ (two-sided) was considered to be statistically significant. Univariable analysis was applied to assess the clinical baseline data.

Results

Clinical characteristics

In this study, the training cohort included 94 patients (mean age, 64.19 ± 8.32 years old; range, 43–83 years old), with 74 males and 20 females, and the validation cohort consisted of 40 patients (mean age, 61.23 ± 9.57 years old; range, 40–84 years old), with 31 males and 9 females. There were no statistically significant differences in age, sex, clinical stage, and CT-reported T stage between HER2-positive and HER2-negative patients in the training and validation cohorts ($P > 0.05$). The differences in CEA level were statistically significant between the HER2-

positive and HER2-negative patients in the training cohort ($P=0.002$) but not in the validation cohort ($P=0.174$). More details are shown in *Table 1*.

Radiomics feature selection and radiomics signature building

In total, 12,410 radiomics features were extracted from each VOI. Next, 7,185 radiomics features with ICCs >0.75 were selected for further analysis. Among these, a total of 1,250 radiomics features remained after excluding features with high correlation. By using the LASSO logistic regression method with five-fold cross-validation, seven radiomics features were selected to calculate the Rad-score for each patient with gastric cancer. Details of the selected features are shown in *Supplementary Table S2*. Subsequently, a radiomics signature was built in the training cohort (*Figure 2*).

Predictive performance of radiomics signature

A significant difference was observed in the Rad-scores between the HER2-positive and HER2-negative patients in the training cohort ($P<0.001$), which was then verified in the validation cohort ($P=0.023$). The mean Rad-score in patients with HER2-positive gastric cancer was significantly higher than that in the HER2-negative group in both cohorts. The AUC of the radiomics signature was 0.782 [95% confidence interval (95% CI): 0.686–0.879] in the training cohort and 0.736 (95% CI: 0.554–0.918) in the validation cohort, respectively (*Figure 3*).

Construction of nomogram

In the univariate analysis, the radiomics signature and CEA level were associated with HER2 status. Multivariable logistic regression analysis identified the CEA level and radiomics signature as independent predictors (*Table 2*).

Table 1 Characteristics of patients in training and validation cohorts

Characteristics	Training cohort [n (%)]		P	Validation cohort [n (%)]		P
	HER2-	HER2+		HER2-	HER2+	
Age ($\bar{x}\pm s$) (year)	64.61 \pm 8.39	63.38 \pm 8.25	0.497	59.20 \pm 8.87	64.60 \pm 10.03	0.084
Sex			0.336			0.379
Male	47 (75.8)	27 (84.4)		21 (84.0)	10 (66.7)	
Female	15 (24.2)	5 (15.6)		4 (16.0)	5 (33.3)	
CEA level			0.002			0.174
Normal	54 (87.1)	19 (59.4)		23 (92.0)	11 (73.3)	
Abnormal	8 (12.9)	13 (40.6)		2 (8.0)	4 (26.7)	
Tumor location			0.937			0.027
Upper-third	19 (30.6)	10 (31.2)		5 (20.0)	8 (53.3)	
Middle-third	10 (16.1)	6 (18.8)		7 (28.0)	0 (0)	
Lower-third	33 (53.2)	16 (50.0)		13 (52.0)	7 (46.7)	
Clinical stage			0.109			0.229
I	18 (29.0)	5 (15.6)		5 (20.0)	6 (40.0)	
II	19 (30.6)	6 (18.8)		7 (28.0)	1 (6.7)	
III	24 (38.7)	20 (62.5)		12 (48.0)	8 (53.3)	
IV	1 (1.6)	1 (3.1)		1 (4.0)	0 (0)	
CT-reported T stage			0.140			0.476
T1–2	25 (40.3)	8 (25.0)		6 (24.0)	6 (40.0)	
T3–4	37 (59.7)	24 (75.0)		19 (76.0)	9 (60.0)	
Rad-score ($\bar{x}\pm s$)	-0.761 \pm 0.235	-0.501 \pm 0.248	<0.001	-0.762 \pm 0.227	-0.534 \pm 0.316	0.023

CEA, carcinoembryonic antigen; CT, computed tomography; HER2, human epidermal growth factor receptor 2; HER2-, HER2-negative patients; HER2+, HER2-positive patients; Rad-score, radiomics score. P value was calculated with the univariable association analysis between each of the clinical variables and HER2 status.

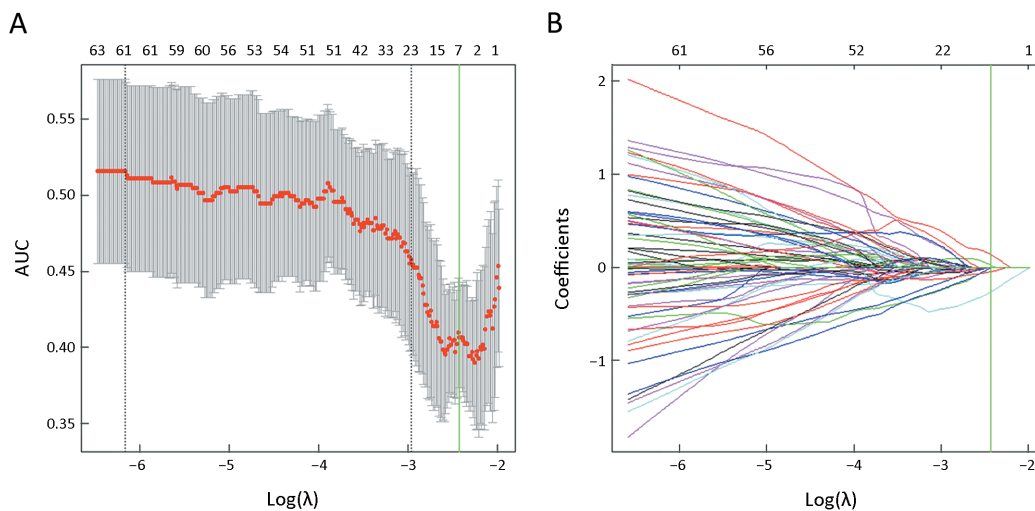


Figure 2 Feature selection with the least absolute shrinkage and selection operator (LASSO) binary logistic regression model. (A) Tuning parameter (λ) selection of LASSO model. The area under curve (AUC) was drawn versus $\log(\lambda)$. Vertical green lines were plotted at the best value with using 5-fold cross-validation to tune parameter (λ) selection in the LASSO model; (B) LASSO coefficient profiles of the features. Each colored line represents corresponding coefficient of each feature. Vertical green line was drawn at the selected λ , where nonzero coefficients were obtained with 7 features.

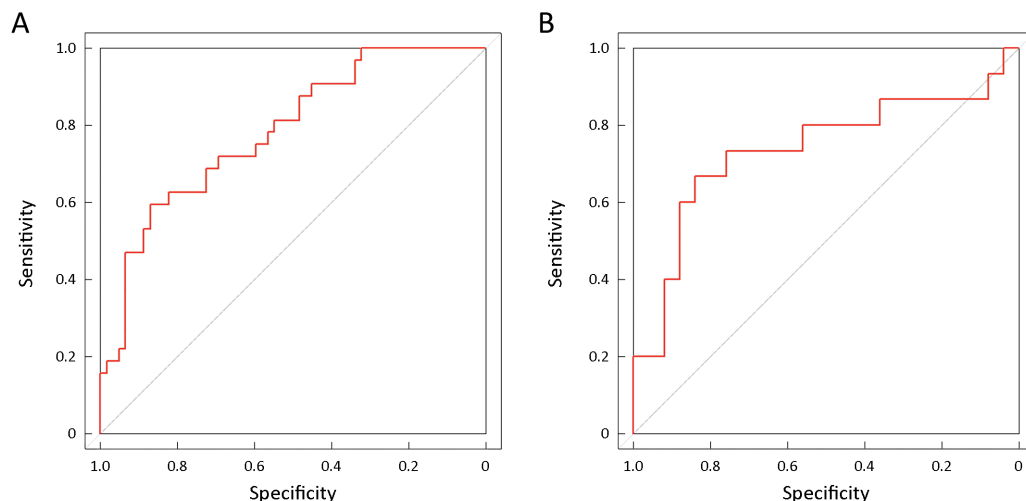


Figure 3 Receiver operating characteristic (ROC) curves of radiomics signature in training cohort (AUC: 0.782, 95% CI: 0.686–0.879) (A) and validation cohort (AUC: 0.736, 95% CI: 0.554–0.918) (B). AUC, area under the curve; 95% CI, 95% confidence interval.

The CEA level was integrated into the nomogram with the radiomics signature in the training cohort (Figure 4).

Predictive performance of radiomics nomogram

The radiomics nomogram demonstrated good discriminative performance for HER2 status prediction in the training cohort (AUC: 0.799; 95% CI: 0.704–0.894) and in the validation cohort (AUC: 0.771; 95% CI:

0.607–0.934). The calibration curve of the radiomics nomogram showed good agreement between the observed outcome and prediction in both training and validation cohorts (Figure 5). The DCA for the radiomics nomogram of the training cohort is presented in Figure 6, and it showed a greater net benefit than the treat-all-patients or the treat-none schemes at the threshold probability of 20%–90%. Moreover, the addition of the CEA level to the prediction model along with radiomics signature

Table 2 Predictors for HER2 status in gastric cancer

Intercept and variables	β	OR (95% CI)	P
Intercept	1.726	–	0.024
Radiomics signature	4.272	4.838 (2.094–11.177)	<0.001
CEA level	1.270	3.559 (1.152–10.992)	0.027

CEA, carcinoembryonic antigen; β , the regression coefficient; OR, odds ratio; 95% CI, 95% confidence interval.

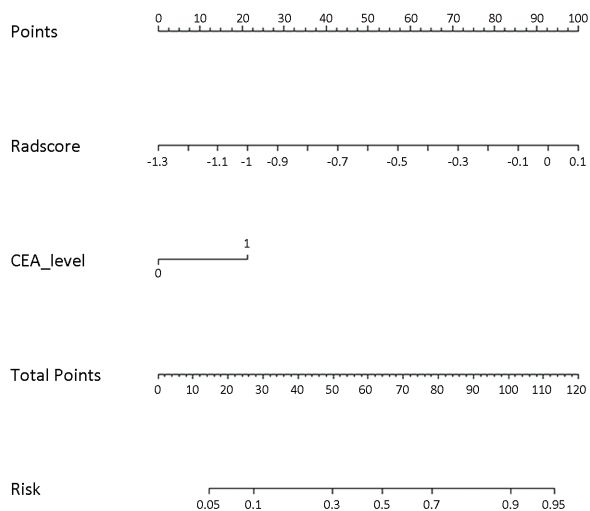


Figure 4 Developed radiomics nomogram. The radiomics nomogram was built in the training cohort, with the radiomics signature and carcinoembryonic antigen (CEA) level incorporated. The CEA level was considered as 0 when the CEA value ≤ 5 ng/mL and considered as 1 when the CEA value > 5 ng/mL.

significantly improved the prediction performance in the training cohort (NRI, 0.889; $P < 0.001$; event NRI, 0.438; nonevent NRI, 0.452) and validation cohort (NRI, 0.853; $P = 0.004$, event NRI, 0.243; nonevent NRI, 0.520).

Discussion

In this study, we developed and validated a CT-based radiomics nomogram for preoperative prediction of HER2 status in patients with pre-treatment gastric cancer. The nomogram, which consisted of the radiomics signature and CEA level, successfully stratified patients according to HER2 status and showed good performance in both cohorts.

The discrimination of accurate HER2 status plays an essential role in the management of unresectable advanced HER2-positive gastric cancer, which can be treated with targeted therapy using trastuzumab (10). Gastroscopic biopsy is routinely applied to diagnose gastric cancer and

test for HER2 status, but gastroscopy can cause some side effects, such as bleeding, gastric perforation, and infection (27). Most previous studies have investigated the relationship between image characteristics and HER2 status in gastric cancer by using ^{18}F -fluorodeoxyglucose (^{18}F -FDG) PET/CT imaging. Park *et al.* (12) and Chen *et al.* (13) found that ^{18}F -FDG PET/CT may allow prediction of the HER2 status of gastric cancer, but the two studies provided contradicting accounts of the association between the maximum standardized uptake value (SUV) and HER2 status. In comparison with these studies, our study showed a better predictive performance in both training and validation cohorts. Moreover, ^{18}F -FDG PET/CT is more expensive and less frequently used in clinical practice than CT. Since contrast-enhanced CT was more commonly applied in tumor management, CT textural analysis has been utilized to predict histopathological characteristics and immunohistochemical biomarkers in gastric cancer (28,29). With regard to the use of CT-based radiomics for predicting genetic status, although several studies have reported the findings of other malignant cancers (30,31), to our knowledge, no previous study had reported the findings of gastric cancer. Our study demonstrated that a CT-based radiomics approach has the potential to predict HER2 status in gastric cancer.

In addition, some studies have explored the association between CEA level and HER2 status. Chen *et al.* (32) found that the serum CEA level alone was not associated with HER2 overexpression, while Park *et al.* (33) reported that the median serum CEA level was associated with HER2 status. Owing to the inconsistent conclusions above, we also performed further analysis in this study. We found that the CEA level showed added value in HER2 prediction by comparing the performance of radiomics nomogram and signature in the training cohort (NRI, 0.889; $P < 0.001$; event NRI, 0.438; nonevent NRI, 0.452) and the validation cohort (NRI, 0.853; $P = 0.004$; event NRI, 0.243; nonevent NRI, 0.520).

There are some limitations in our study. First, the sample size of this retrospective study was relatively small. However, our study provided pioneering results

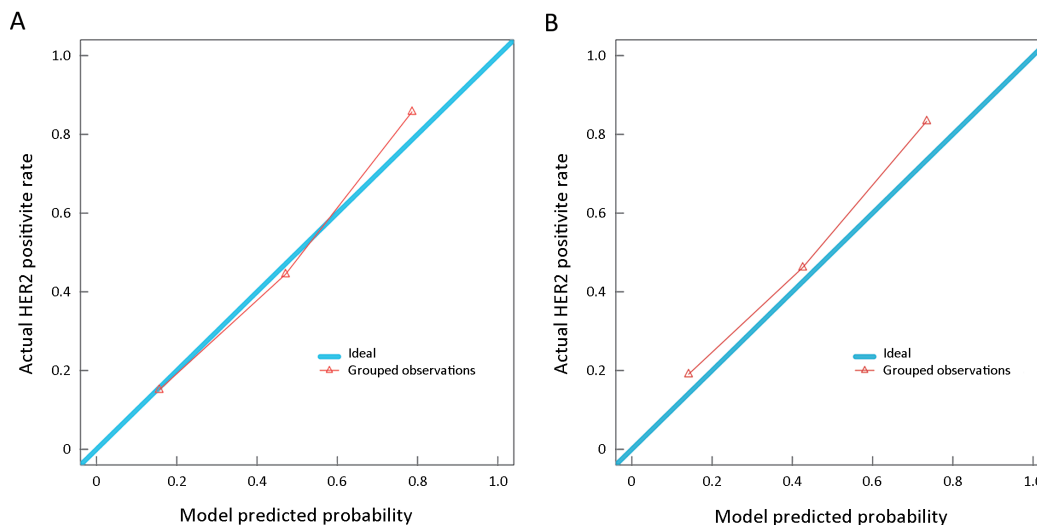


Figure 5 Calibration curves of radiomics nomogram in training and validation cohorts. Calibration curve plots demonstrate the calibration between predicted risks of human epidermal growth factor receptor 2 (HER2)-positive status and observed outcomes of HER2-positive status in the training cohort (A) and the validation cohort (B).

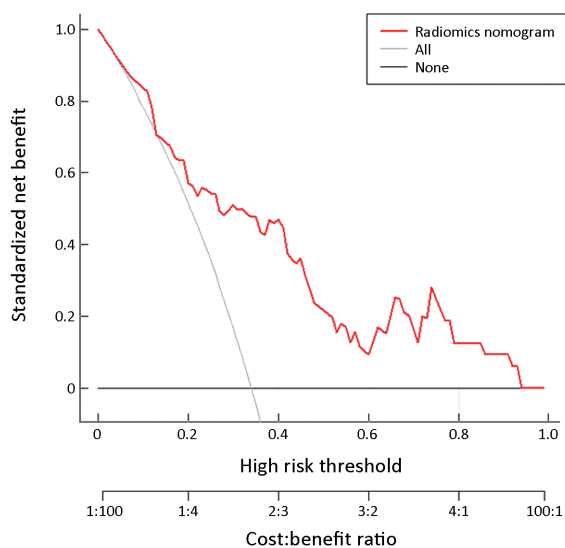


Figure 6 Decision curve analysis (DCA) for radiomics nomogram in training cohort. The vertical axis displays standardized net benefit. The two horizontal axes show the correspondence between risk threshold and cost:benefit ratio.

demonstrating the potential of radiomics in the prediction of HER2 status in gastric cancer. Therefore, prospective and multi-center external validation with larger sample sizes is warranted to further validate and improve the performance of our proposed radiomics signature. Second, the radiomics features used in this study were only extracted from the portal venous phase CT images. This was because differentiation of the tumor from the adjacent

normal gastric tissue was maximal in the portal venous phase, and other phases should be investigated in future.

Conclusions

Our study presents a prediction nomogram that consists of the preoperative CEA level and CT-based radiomics signature, and could be conveniently used for preoperative individualized prediction of the HER2 status in patients with pre-treatment gastric cancer.

Acknowledgements

This work supported by the National Key Research and Development Program of China (No. 2017YFC1309100), National Natural Scientific Foundation of China (No. 81771912, 81601469, and 81701782), the Science and Technology Planning Project of Guangdong Province (No. 2017B020227012), and the Science and Technology Planning Project of Guangzhou (No. 20191A011002).

Footnote

Conflicts of Interest: The authors have no conflicts of interest to declare.

References

1. Bray F, Ferlay J, Soerjomataram I, et al. Global cancer statistics 2018: GLOBOCAN estimates of incidence

- and mortality worldwide for 36 cancers in 185 countries. *CA Cancer J Clin* 2018;68:394-424.
2. World Health Organization. World Cancer Report 2014. 150 cours Albert Thomas, 69372. Lyon: International Agency for Research on Cancer, 2014.
 3. Chen W, Sun K, Zheng R, et al. Cancer incidence and mortality in China, 2014. *Chin J Cancer Res* 2018; 30:1-12.
 4. Ajani JA, D'Amico TA. NCCN Clinical Practice Guidelines in Oncology-Gastric Cancer (Version 2. 2019): National Comprehensive Cancer Network, 2019.
 5. Miao RL, Wu AW. Towards personalized peri-operative treatment for advanced gastric cancer. *World J Gastroenterol* 2014;20:11586-94.
 6. Orditura M, Galizia G, Sforza V, et al. Treatment of gastric cancer. *World J Gastroenterol* 2014;20: 1635-49.
 7. Boku N. HER2-positive gastric cancer. *Gastric Cancer* 2014;17:1-12.
 8. Bang YJ, Van Cutsem E, Feyereislova A, et al. Trastuzumab in combination with chemotherapy versus chemotherapy alone for treatment of HER2-positive advanced gastric or gastro-oesophageal junction cancer (ToGA): a phase 3, open-label, randomised controlled trial. *Lancet* 2010;376:687-97.
 9. Gravalos C, Jimeno A. HER2 in gastric cancer: a new prognostic factor and a novel therapeutic target. *Ann Oncol* 2008;19:1523-9.
 10. CUREA FG, Hebbbar M, Ilie SM, et al. Current targeted therapies in HER2-positive gastric adenocarcinoma. *Cancer Biother & Radiopharm* 2017;32:351-63.
 11. Hirai I, Tanese K, Nakamura Y, et al. Assessment of the methods used to detect HER2-positive advanced extramammary Paget's disease. *Med Oncol* 2018; 35:92.
 12. Park JS, Lee N, Beom SH, et al. The prognostic value of volume-based parameters using 18F-FDG PET/CT in gastric cancer according to HER2 status. *Gastric Cancer* 2018;21:213-24.
 13. Chen R, Zhou X, Liu J, et al. Relationship between 18F-FDG PET/CT findings and HER2 expression in gastric cancer. *J Nucl Med* 2016;57:1040-4.
 14. Amin MB, Edge SB, Greene FL, et al. *AJCC Cancer Staging Manual*. 8th Edition. New York: Springer, 2016.
 15. Gevaert O, Xu J, Hoang CD, et al. Non-small cell lung cancer: identifying prognostic imaging biomarkers by leveraging public gene expression microarray data--methods and preliminary results. *Radiology* 2012;264:387-96.
 16. Coroller TP, Agrawal V, Huynh E, et al. Radiomic-based pathological response prediction from primary tumors and lymph nodes in NSCLC. *J Thorac Oncol* 2017;12:467-76.
 17. Lambin P, Rios-Velazquez E, Leijenaar R, et al. Radiomics: extracting more information from medical images using advanced feature analysis. *Eur J Cancer* 2012;48:441-6.
 18. Gillies RJ, Kinahan PE, Hricak H. Radiomics: Images are more than pictures, they are data. *Radiology* 2016;278:563-77.
 19. Li Z, Zhang D, Dai Y, et al. Computed tomography-based radiomics for prediction of neoadjuvant chemotherapy outcomes in locally advanced gastric cancer: A pilot study. *Chin J Cancer Res* 2018;30: 406-14.
 20. Jiang Y, Chen C, Xie J, et al. Radiomics signature of computed tomography imaging for prediction of survival and chemotherapeutic benefits in gastric cancer. *EBioMedicine* 2018;36:171-82.
 21. Li W, Zhang L, Tian C, et al. Prognostic value of computed tomography radiomics features in patients with gastric cancer following curative resection. *Eur Radiol* 2019;29:3079-89.
 22. Yoon SH, Kim YH, Lee YJ, et al. Tumor heterogeneity in human epidermal growth factor receptor 2 (HER2)-positive advanced gastric cancer assessed by CT texture analysis: Association with survival after trastuzumab treatment. *PloS One* 2016; 11:e0161278.
 23. Tsurumaru D, Miyasaka M, Nishimuta Y, et al. Differentiation of early gastric cancer with ulceration and resectable advanced gastric cancer using multiphasic dynamic multidetector CT. *Eur Radiol* 2016;26:1330-7.
 24. Huang YQ, Liang CH, He L, et al. Development and validation of a radiomics nomogram for preoperative prediction of lymph node metastasis in colorectal cancer. *J Clin Oncol* 2016;34:2157-64.
 25. Song J, Shi J, Dong D, et al. A new approach to predict progression-free survival in stage IV EGFR-

- mutant NSCLC patients with EGFR-TKI therapy. *Clin Cancer Res* 2018;24:3583-92.
26. Konigsberg B, Hess R, Hartman C, et al. Inter- and intraobserver reliability of two-dimensional CT scan for total knee arthroplasty component malrotation. *Clin Orthop Relat Res* 2014;472:212-7.
 27. Levy I, Gralnek IM. Complications of diagnostic colonoscopy, upper endoscopy, and enteroscopy. *Best Pract Res Clin Gastroenterol* 2016;30:705-18.
 28. Liu S, Liu S, Ji C, et al. Application of CT texture analysis in predicting histopathological characteristics of gastric cancers. *Eur Radiol* 2017;27:4951-59.
 29. Liu S, Shi H, Ji C, et al. CT textural analysis of gastric cancer: correlations with immunohistochemical biomarkers. *Sci Rep* 2018;8:11844.
 30. Liu Y, Kim J, Balagurunathan Y, et al. Radiomic features are associated with EGFR mutation status in lung adenocarcinomas. *Clin Lung Cancer* 2016;17:441-48.e6.
 31. Yang L, Dong D, Fang M, et al. Can CT-based radiomics signature predict KRAS/NRAS/BRAF mutations in colorectal cancer? *Eur Radiol* 2018;28:2058-67.
 32. Chen XZ, Zhang WH, Chen HN, et al. Associations between serum CA724 and HER2 overexpression among stage II-III resectable gastric cancer patients: an observational study. *Oncotarget* 2016;7:23647-57.
 33. Park JS, Rha SY, Chung HC, et al. Clinicopathological features and prognostic significance of HER2 expression in gastric cancer. *Oncology* 2015;88:147-56.

Cite this article as: Li Y, Cheng Z, Gevaert O, He L, Huang Y, Chen X, Huang X, Wu X, Zhang W, Dong M, Huang J, Huang Y, Xia T, Liang C, Liu Z. A CT-based radiomics nomogram for prediction of human epidermal growth factor receptor 2 status in patients with gastric cancer. *Chin J Cancer Res* 2020;32(1):62-71. doi: 10.21147/j.issn.1000-9604.2020.01.08

Table S1 CT scanning parameters for patients

Scanner	Tube voltage (kV)	Tube current (mAs)	Rotation time (s)	Detector collimation (mm)	Field of view (mm)	Matrix	Reconstruction section thickness (mm)	Acquisition time (s)	
								Arterial phase	Portal venous phase
SOMATOM Definition Flash (Siemens Healthcare, Forchheim, Germany)	120	130	0.5	2×64×0.6	360×360	512×512	1.0	30	60
256-slice Brilliance iCT (Philips Healthcare, Cleveland, Ohio, USA)	120	130	0.5	128×0.625	360×360	512×512	1.0	30	60
64-slice LightSpeed VCT (GE Medical systems, Milwaukee, WI, USA)	120	130	0.4	64×0.625	360×360	512×512	1.25	30	60

CT, computed tomography.

Table S2 Characteristics of selected features in radiomics signature

Features	Mean	Standard deviation
db4_3_skewness	0.114	0.380
db10_7_GLSZM_LALGLE	27.973	75.626
bior5.5_7_GLDM_SDHGLE	50.785	15.672
bior5.5_8_kurtosis	3.581	0.645
rbio2.2_1_GLCM_correlation	0.872	0.050
rbio2.8_1_GLSZM_SALGLE	0.007	0.004
rbio3.1_2_GLDM_DE	6.254	0.416

Supplementary materials

Feature analysis methodology

Feature analysis was applied to the computed tomography (CT) images using in-house feature analysis software with algorithms implemented in Matlab 2016b (Math-works, Natick, MA, USA). The CT images of these lesions were resampled with a pixel size of 1 mm × 1 mm × 1.25 mm using linear interpolation and then separately normalized with min-max normalization to convert the pixels from -300 HU to 700 HU into a range of (1, 100) of integral intensities.

Wavelet features

These features were extracted from an image after decomposing by different wavelets. Different functions (high-pass or low-pass, represented by H or L) on different scale (X, Y, Z) were represented by a number from 1 to 8 (LLL, LLH, LHL, LHH, HLL, HLH, HHL, HHH).

Wavelet decomposition should follow the formula:

$$X'(i, j, k) = \sum_p^{N_x} \sum_q^{N_y} \sum_r^{N_z} H_x(p) H_y(q) H_z(r) X(i + p, j + q, k + z)$$

The following wavelets were used:

db1,db4,db7,db10,sym7,sym8,coif1,coif5,bior2.2,bior2.8,bior3.1,bior3.7,bior5.5, bior6.8, rbio2.2, rbio2.8, rbio3.1, rbio3.7, rbio5.5, rbio6.8.

From the image reconstructed, the first order statistic and texture features were extracted. A prefix including wavelet name and the number representing function were added to the features' names.

Feature generation

A series of gray-level histogram features and texture features were generated from the image with and without wavelet transform. When calculating texture features, the volume of interest (VOI) was resampled using a bin number of 25.

Formula of features were in <https://pyradiomics.readthedocs.io/en/latest/> or “Image biomarker standardisation initiative - feature definitions” (1).

Use of R packages

The “glmnet” package was used for least absolute shrinkage and selection operator (LASSO) logistic regression analysis. The receiver operating characteristic (ROC) plots of radiomics signature were performed with the “pROC” package. The multivariable logistic regression analysis and calibration plots were done with the “rms” package. The “rmda” package was applied for decision curve analysis (DCA). And the “Hmisc” package was utilized to calculate the net reclassification improvement (NRI).

Formula of radiomics signature

Rad-score= $-0.672324822-0.047261970*\text{db4_3_skewness}-0.005949972*\text{db10_7_GLSZM_LALGLE}+0.138440603*\text{bior5.5_7_GLDM_SDHGLE}+0.023320530*\text{bior5.5_8_kurtosis}-0.002511368*\text{rbio2.2_1_GLCM_correlation}-0.001464398*\text{rbio2.8_1_GLSZM_SALGLE}-0.264647243*\text{rbio3.1_2_GLDM_DE}$

References

1. Zwanenburg A, Leger S, Vallières M, et al. Image biomarker standardization initiative. arXiv preprint arXiv:1612.07003.